

Experimental study of inlet effects on mass transport in electrochemical filter–press parallel reactors

G. Rodríguez^a, F.Z. Sierra-Espinosa^{b,*}, A. Álvarez^b, F. Carrillo^a

^aCentro de Investigación en Ingeniería y Ciencias Aplicadas, CIICAp, Universidad Autónoma del Estado de Morelos, UAEM, Av. Universidad 1001, Col. Chamilpa, Cuernavaca, C.P. 62209 Morelos, México

^bCentro de Investigación en Ingeniería y Ciencias Aplicadas, CIICAp, Universidad Autónoma del Estado de Morelos, UAEM, Av. Universidad 1001, Col. Chamilpa, Cuernavaca, C.P. 62209 Morelos, México, Tel. +52 777 329 7084, Fax +52 777 329 7984, e-mail: fse@uaem.mx (F.Z. Sierra)

Received 23 June 2016; Accepted 17 November 2016

ABSTRACT

Electrochemical reactors are widely used for water treatment in many industrial processes, including removal of bacteria and other living organisms. This paper analyzes the effects of inlet configuration in filter-press parallel plate channel reactors using computational fluid dynamics, CFD. The numerical model was validated using experimental data of velocity obtained by particle image velocimetry, PIV. The parallel plates of the channel are 10 mm apart from each other to form a confined domain with diverging-converging sections inlet-outlet of angles of 19.3°/30.3°, respectively. This geometry configuration produces a flow distribution, which cannot be considered as fully, developed flow. A numerical solution of the transport governing equations linked together to electro chemistry was obtained for calculating the total flux of ions, between the electrolyte and the cathode. Properties of hydrated copper sulfate ($\text{CuSO}_4 + 5\text{H}_2\text{O}$) compound simulating an electro deposit process were considered. A range of flow Reynolds number was studied. The results show evidence that modifying the inlet configuration provide different flow patterns, improving the effectivity of the reactor. Measurements and predictions of velocity do agree, showing strong velocity gradients with more than one inflexion point and vortex are eliminated from the reactor, which improve its efficiency. The results of km profiles along the reactor were compared using both the measured velocity field and the predicted velocity, demonstrating the impact of inlet configuration. By comparing the results against the results reported for the FM01-LC electrolyser it is demonstrated that the present configuration is widely competitive.

Keywords: Channel flow; PIV; CFD; Electrochemical reactor; Inlet configuration effects

1. Introduction

Electrochemical reactors have been considered for use in many applications in recent years [1–3]. The production of hydrogen [4] and water treatment are among the most promising [5–7]. For these goals, parallel plates filter press reactors are gaining the attention because their simplicity of configuration and operation. This reactor

exposes a cathode in contact to an electrolyte that flows between the two parallel plates at moderate Reynolds number. However, the electrolyte dynamic flow defines the effectivity of the required chemical reaction between the electrolyte and the electrode [8]. This is because the design of the reactors considers average values of electrolyte velocity to quantify the mass transport k_m . Therefore, electrolyte behavior not in fully developed flow condition affects the process [9].

*Corresponding author.

Presented at the EDS conference on Desalination for the Environment: Clean Water and Energy, Rome, Italy, 22–26 May 2016.

It has been observed that the flow distribution in the reactor is sensitive to design details like the configuration of inlet section. By modifying the geometry of inlet section or even its orientation it is possible to modify the flow structure between the parallel plates, in order to obtain a flow that approximates the fully developed condition [10]. A parallel plate reactor may enhance through a systematic study of inlet geometry, which can be obtained by designing the reactor using computational fluid dynamics, CFD. This approach allows the designer considering the velocity conditions at the proximity of the cathode's surface, where chemical reactions are taking place, instead of using average quantities [11]. However, the more uniform the flow the more efficient the reactor, no matter what approach the design is based on. Therefore, the present investigation focuses on analyzing different flow conditions in the reactor caused by inlet geometry modifications. The objective was to define the best inlet configuration in terms of mass transport and molar concentration in the surface of the cathode. Results obtained with a proposed reactor that incorporates an inlet perpendicularly aligned to the reactor's axis compared well against the performance of a commercial electrochemical reactor known as FM01-LC [12,13].

2. Configuration under study

First we present the modifications to the inlet reactor under analysis. The present reactor is 100 mm length and 50 mm wide in its rectangular section. The numerical solution considers a cathode lies on the surface of one plate to be in contact with the moving electrolyte. The separation between the upper and lower plates is of 10 mm. A fundamental description of the reactor as well as more construction details were given elsewhere [10,11].

2.1. Inlet geometry of reactor

The modifications to the inlet configuration included the shape and orientation of the pipe, as can be observed in Fig. 1a–c. Configuration number 1 is shown in Fig. 1a, where the cross section of inlet pipe of diameter 13.7 mm was partially sectioned on the top and bottom. Configuration number 2 consists of a non-sectioned but reduced pipe diameter to 9.5 mm, see Fig. 1b. Configuration num-

ber 3 is of diameter 6.35 mm, oriented axially perpendicular to the reactor's axis, as shown in Fig. 1c. The reactor including this last modification is observed in the picture of Fig. 1d.

The exit pipe orientation of the reactor in all three cases was perpendicular to reactor's axis, as indicated by arrowed exit in Fig. 1c. A comparison of results showed the advantage of configuration number 3, therefore this paper focuses on the flow distribution obtained with this option. While the FM01-LC electrolyser produces a fully developed flow by using a manifold flow distributor [13], the flow in configuration number 3 aligns in the axial direction. Therefore an advantage of present reactor's compared against the FM01-LC is its simplicity of construction.

2.2. Experimental set-up

In this work the velocity field in the channel reactor was measured using particle image velocimetry, PIV. This is considered an accurate and reliable technique for studying vortex dynamics in laminar and turbulent flows [14,15]. In PIV, particles seeded artificially follow the streams allowing a detailed description of the fluid motion. Particle displacement defines the velocity magnitude and direction of fluid by digitalizing laser light spots reflected by these particles in an illuminated plane. In this case, the illuminated plane was located at mid distance of parallel plate separation. Particles of crystal of 50 nm, finished by silver dioxide, reflected part of the laser light from two pulses elapsed a time interval, $t = 10.3$ ms. Cross-correlation was used to validate the information from the particle position allowing averaging the flow velocity in a number of interrogation areas of 32×32 pixels [16,17]. Table 1 presents the PIV settings used during the experimental measurements.

Table 1
Experimental set up for PIV measurements

Parameter	Units	Magnitude
Scale factor	non dimensional	13.457
Interrogation area	pixel	32×32
Time elapsed	μs	10.3
Repetition rate	Hz	15
Particle size	μm	50

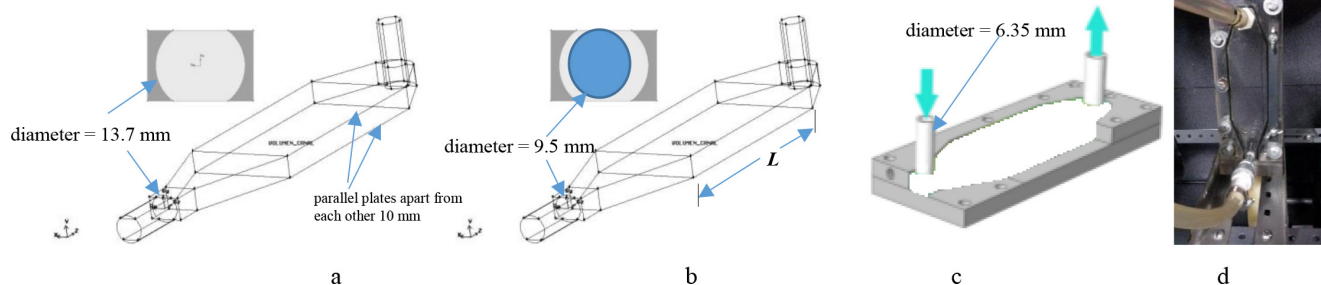


Fig. 1. Filter press parallel plates reactor under analysis; a) Schematic of reactor with main dimensions; L is the region of electrochemical reaction; a) Configuration number 1, sectioned inlet pipe, aligned to the reactor axially; b) Configuration 2, reduced diameter of inlet pipe; c) Configuration 3, proposed parallel plate reactor with perpendicular inlet pipe; d) Front photograph of reactor.

2.3. Numerical simulation

Finite volume is an approach used to solve algebraically the mass and momentum transport equations by computational fluid dynamics, CFD. This technique discretizes a domain that represents computationally the flow, where partial differential equations are solved, such that pressure, velocity and electrochemical reactions are calculated in detail for specific boundary conditions. The present work used a commercial program Comsol to solve the transport equations that govern a copper sulfate electrolyte, moving in contact with the cathode that lies in one of the parallel plates of the reactor. A mass flow 0.025 kg s^{-1} get into the reactor shown in Figs. 1a–c. The solution assumed a Newtonian, incompressible flow in steady state. The no-slip condition was applied to the walls of the reactor. The reader can consult published literature for details on equations and Reynolds Averaged Navier-Stokes equations, RANS, method used in this investigation [18].

A flow that produces an electrochemical reaction of ion motion from the electrolyte as a function of diffusion, migration and convection. The flux or mass transport of the electroactive species i [1] is:

$$N_{Cu^{2+}} = -\left(D_{Cu^{2+}} + Dt_{Cu^{2+}}\right) \cdot \frac{\partial}{\partial x_i} C_{Cu^{2+}} - \frac{z_i F}{RT} D_{Cu^{2+}} C_{Cu^{2+}} \frac{\partial}{\partial x_i} \phi + u_i \cdot C_{Cu^{2+}} \quad (1)$$

where last term links electrochemical activity with flow condition through the velocity field expressed by u_i . Sub-index cu^{2+} accounts for cupric ions (Cu^{2+}); D represents cupric ions diffusion coefficient; D_i expresses diffusion affected by turbulence; R is the molar gas constant; F is Faraday constant; z_i is a charge of species i at temperature T ; ϕ is electric field causing mass transfer by migration; finally u is the local velocity computed from the momentum equation, which is given elsewhere [11]. In Eq. (1) the migration effect is neglected by adding an excess of supporting electrolyte to the solution. Thus, it reduces to:

$$N_{Cu^{2+}} = -\left(D_{Cu^{2+}} + Dt_{Cu^{2+}}\right) \cdot \frac{\partial}{\partial x_i} C_{Cu^{2+}} + u_i \cdot C_{Cu^{2+}} \quad (2)$$

The analogy between heat and mass transport due to diffusion in a turbulent flow, Dt , Kays-Crawford [19], involve turbulent Prandtl and Schmidt numbers equality:

$$Dt_{Cu^{2+}} = \frac{\mu_t}{\rho Sc_t} \quad (3)$$

where the turbulent Schmidt number is defined as:

$$Sc_t = \left(\frac{1}{2Sc_{t\infty}} + \frac{0.3 \cdot \mu_t}{\sqrt{Sc_{t\infty}} \cdot \rho \cdot D_i} - \left(\frac{0.3 \cdot \mu_t}{\rho \cdot D_i} \right) \cdot \left(1 - \exp\left(-\frac{\rho \cdot D_i}{0.3 \cdot \mu_t \cdot \sqrt{Sc_{t\infty}}} \right) \right) \right)^{-1} \quad (4)$$

with $Sc_{t\infty}$ a constant equal to 0.85 [19].

Solving the velocity field near the cathode surface allowed the calculation of a mass transport coefficient k_m as:

$$k_{mCFD} = \frac{J_c}{Z_i \cdot F \cdot C_i} \quad (5)$$

In Eq. (5) J_c is a density of current in $A m^{-2}$; z_i is the copper ion charge; F represents Faraday's constant, $F = 96485 A s$

mol^{-1} ; and C_i accounts for concentration of electroactive species, where $C_i = 10 \text{ mol m}^{-3}$. In Eq. (5) the density of current in terms of mass transport N_i , gives:

$$J_c = Z_i \cdot F \cdot N_i \quad (6)$$

Therefore, the CFD mass transport coefficient is:

$$k_{mCFD} = \frac{N_i}{C_i} \quad (7)$$

In this work, a k_m coefficient was calculated based on the velocity field, measured with PIV at mid plane of the reactor. The results showed improvement of flow in the electrochemical reactor due to geometry inlet modification. To this end was:

$$k_m = D \left(\frac{Sh}{d_e} \right) \quad (8)$$

$$Sh = a Re^b Sc^c Le^e \quad (9)$$

where Sh , Re , Sc and Le are the Sherwood number, Reynolds number, Schmidt number and the ratio of hydraulic diameter to the length of the electrode in the direction of the flow, respectively; a , b , c and e are empirical constants [1,23]. The validity of Eqs. (8), (9) is limited to fully developed flows; or like the present case, where the proximity to this condition worth their use.

3. Results and discussion

3.1. Flow distribution

Results of velocity measured with PIV for configuration number 1 support the validity of numerical simulations. The results in the form of contours of velocity in the main direction of flow are shown in Fig. 2 a–d for two planes parallel to the reactor's plates, at distances $y = 0.001 \text{ m}$, and $y = 0.005 \text{ m}$ from the bottom. The first two images correspond to the PIV results compared to the CFD results for plane $y = 0.001 \text{ m}$. As observed, the two techniques do agree very well in describing the main stream of the velocity field in the reactor. It consist of one stream of high velocity colored in red, combined with a stream of low velocity, even with negative values of velocity. The results for mid plane, $y = 0.005 \text{ m}$ are shown in Fig. 2c and 2d. Variations of velocity on different planes are due to the effect of the wall, which is higher in the plane near the bottom of the reactor than at mid distance between plates.

The flow field streams extend along the rectangular zone of the reactor of length L . Maximum value of velocity reach $u = 0.12 \text{ m s}^{-1}$ in a small region after the inlet section. As the flow approximates the exit zone on $L = 1$, the velocity decays to less than half the maximum value. The results in the form of streamlines indicate that the streams have characteristics of recirculating flow, as shown by measured and predicted fields in Fig. 3a–d, which compared well. As observed, planes near the bottom and the one at mid plane,

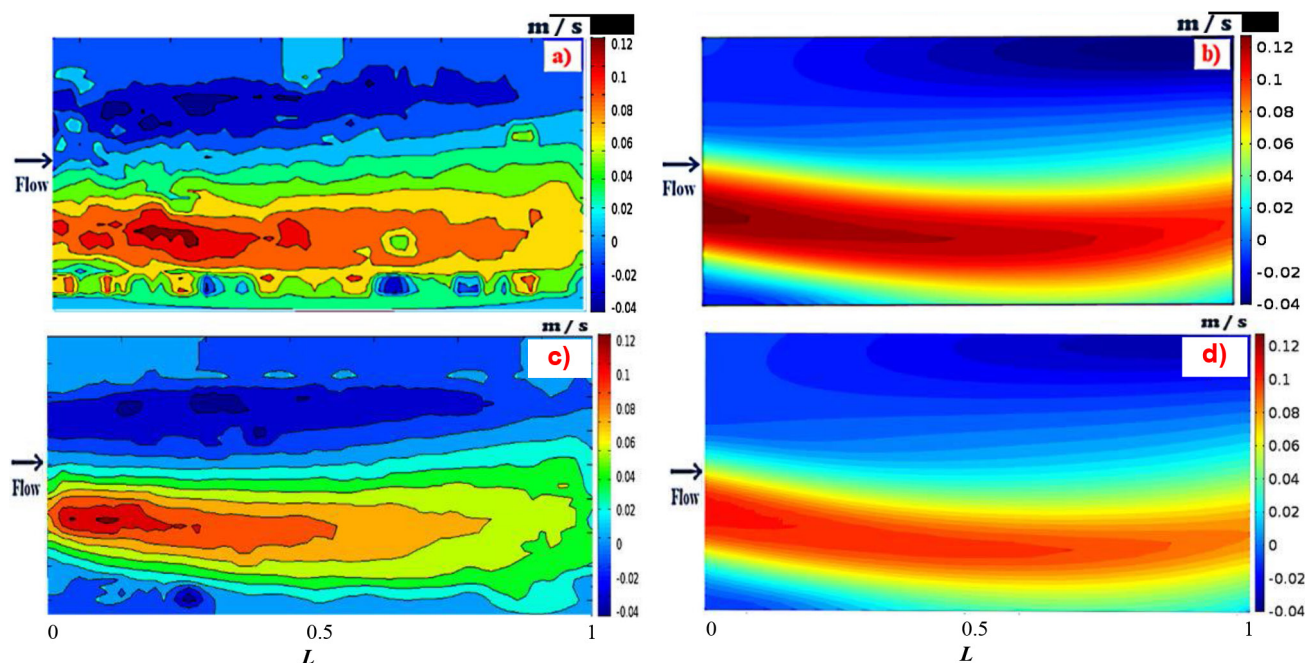


Fig. 2. Comparison of velocity results from CFD to PIV; a) PIV velocity field obtained for plane $y = 0.001$ m; b) CFD velocity field obtained for plane $y = 0.001$ m; c) PIV velocity field obtained for plane $y = 0.005$ m; d) CFD velocity field obtained for plane $y = 0.005$ m.

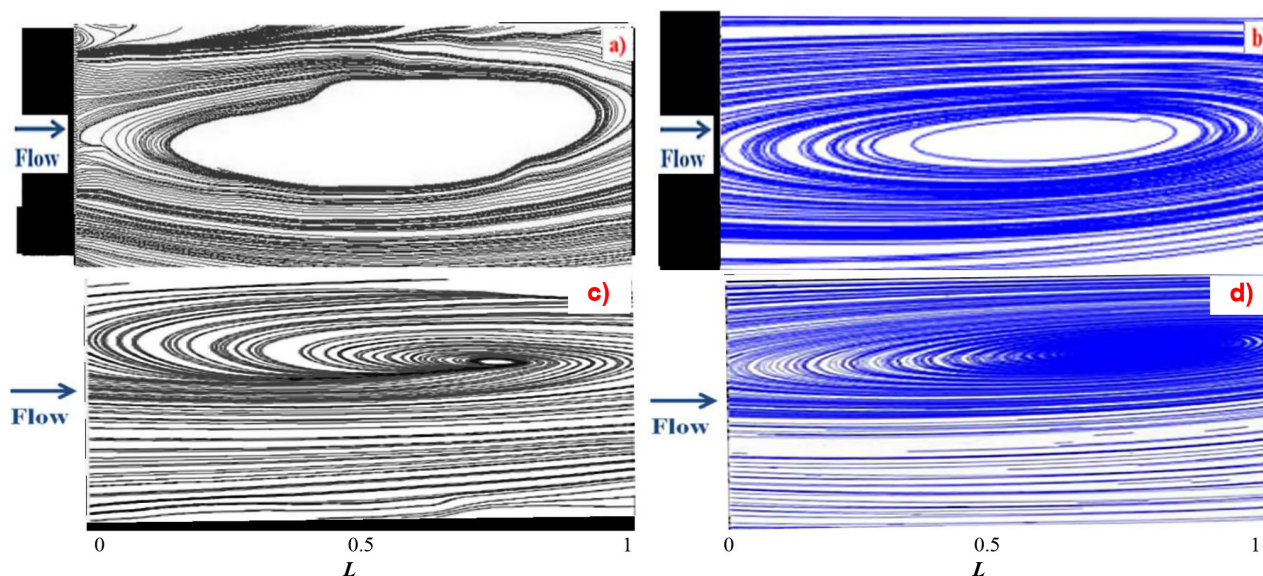


Fig. 3. Comparison of stream lines results, CFD against PIV for inlet pipe axially oriented; a) PIV, plane $y = 0.001$ m; b) CFD, plane $y = 0.001$ m; c) PIV, plane $y = 0.005$ m; d) CFD, plane $y = 0.005$ m.

coincide about the flow distribution, although small differences prevail, confirming the information of the contours of velocity. The recirculating flow and the region of high velocity are far from fully developed, flow condition, which represents an ideal condition for electrochemical applications [12,13]. In this case the flow field is attributed to the divergent geometry of the reactor, which produces an increasing momentum in one section of the domain due to an expansion of the cross section area, while reverse flow balances mass conservation in the cross section area. Reverse flow forms because the exit is convergent, thus the pressure

increases in direction towards the exit, while velocity slows down. The combined effects of inlet-outlet divides the flow along the axial direction, as observed in Fig. 3 a–d. The validity of the simulations is based on the agreement of the CFD results compared against the PIV measurement data of Fig. 2a–d and Fig. 3a–d.

3.2. Change of inlet pipe orientation

The results obtained using configuration 2 were not too different from those for configuration number 1. This

result indicated that a diameter reduction of the inlet pipe alone affects very little the flow distribution in the reactor. Instead, by reducing the pipe diameter in combination with a change of inlet orientation, see Fig. 1c and d, produced a flow similar to one for fully developed condition.

Once the inlet was aligned perpendicularly to the axis of the reactor, the flow reorganized to face a 90 degree change of direction. This condition is quite different from the axial expansion due to the divergence of cross area. Therefore, a pressure balance takes place in the divergent region, where pressure loss due to change of direction compensates the expansion due to increasing the cross area. Tests of velocity measurements with PIV varying the flow rate in the reactor proved the flow alignment for configuration 3 as follows. Table 2 presents the conditions for experiments conducted to describing the flow distribution. Reynolds number Re calculation based on Le , see Eq. (9), uses an average velocity. As observed in Table 1, all tests conducted correspond to laminar regime, which still produce recirculating flow as observed in Figs. 2 and 3.

A sample image of particles moving with the fluid obtained with PIV from the rectangular section of the reactor, plane located at $y = 0.005$ m, is presented in Fig. 4 a. The image corresponds to a mass flow rate 0.050 kg s^{-1} . From particle position information, the velocity vectors field was obtained. The results for all conditions studied are shown in Fig. 4b–e. Small differences observed in the vectors may be attributed to several factors among flow rate increments, instabilities due to divergence and contraction of the cross section area. Increments of pressure in the contraction section may alter the flow condition upstream, in the rectangular section, by un-compressibility of the fluid. In general, we observe that vectors describe a flow orientation in the main direction of flow. As observed in Fig. 4e, uniformity of velocity vectors is higher for the last condition.

A streamlines representation makes the fluid behavior more clear, as observed in Fig. 5a and b. The streamlines correspond to the first and second mass flow rate conditions of Table 2. In Fig. 5a we observe two sections with strong velocity gradients located along the lateral wall, while the streams of center line behave well aligned with the reactor axis, z . According to the classical methods for reactor's design presented by Walsh [1], these flow conditions out of fully developed flow lead to wrong calculations of the mass transport coefficient k_m , which is used to evaluate the efficiency of ionic interchange in the reactor. Therefore, describing the fluid dynamics based on streamlines allowed identifying what sections of the

Table 2
Conditions used in experimental measurement

Test	Mass flow rate kg s^{-1}	Viscosity $\text{kg m}^{-1}\text{s}^{-1}$	Density kg m^{-3}	Re
1	33×10^{-3}	1.19×10^{-3}	998	564
2	50×10^{-3}			840
3	67×10^{-3}			1126
4	84×10^{-3}			1411

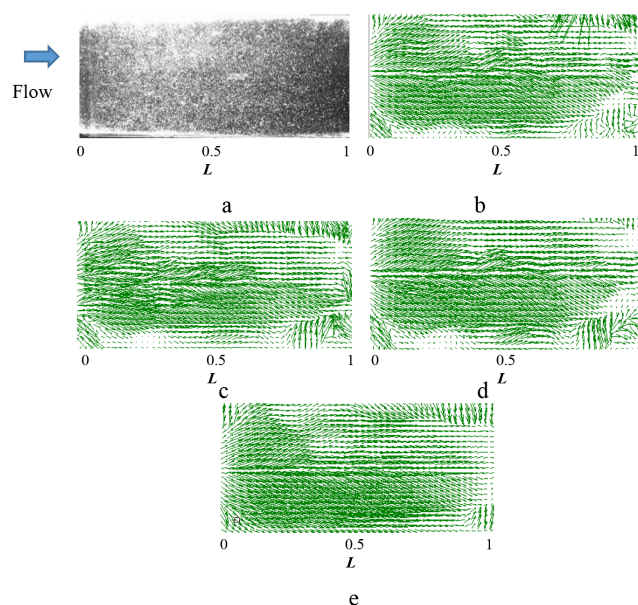


Fig. 4. Results of velocity measurement from PIV for configuration 3, inlet pipe oriented perpendicularly to reactor axis, for plane $y = 0.005$ m; a) Illuminated particle image, sample; b) Velocity vectors for flow 0.033 kg s^{-1} ; c) Velocity vectors for flow 0.05 kg s^{-1} ; d) Velocity vectors for flow 0.067 kg s^{-1} ; e) Velocity vectors for flow 0.0836 .

reactor and what conditions of flow rate produced low reaction efficiency.

Furthermore, the computation of vorticity, indicated where velocity gradients generated vortex motion, which is conceptually opposite to the fully developed flow condition. The regions with higher vortex activity were detected by high intensity color near the lateral walls and

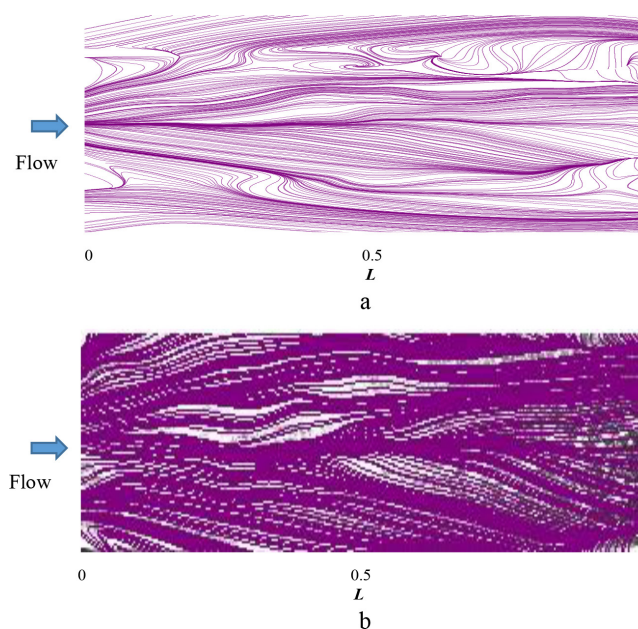


Fig. 5. Stream lines from PIV; a) For flow rate 0.033 kg s^{-1} ; b) For flow rate 0.05 kg s^{-1} .

the center, especially close to the exit region as observed in Fig. 6a and 6b, for first and second conditions of Table 2. By comparing these two flow conditions, we observe that vortex dynamics decrease as Re number increases. Although several spots of vorticity appear over the rest of the flow, their magnitude is doesn't reach the maximum. In order to make this clearer we plotted the velocity magnitude along profiles transversally oriented to the main direction of flow, as observed in Fig. 7a to d. The profiles correspond to five different locations along the distance L .

As observed in Fig. 7a, the first profile on $L = 0$ shows one peak of velocity located on the extreme $x = 1$ of the reactor. This profile shows also several inflexion points where velocity changes magnitude abruptly. As the exit region approaches, the inflexion points reduce and the peak is observed close to $x = 0$, corresponding to profile at $L = 1$. The velocity profiles for next two flow rate conditions depict similar behavior of velocity, except that one

peak appears at $L = 0$, as observed in Fig. 7b and c. Finally, for larger Re number most of profiles at all positions show velocity magnitude with rather soft variation, meaning that the flow aligned in the main direction, as one can see in Fig. 7d. The region from $L = 0.25$ to $L = 0.75$ resulted with more uniform velocity magnitude especially from $x = 0.2$ to $x = 0.8$, which represents a zone of high reaction efficiency, as will be examined below. This result for configuration 3 encouraged a comparison of electrochemical performance against the original configuration, using the capabilities of CFD.

3.3. Numerical prediction of proposed configuration against reactor original design

The flow in configuration 3 was resolved numerically to compare against the converged solution obtained for the

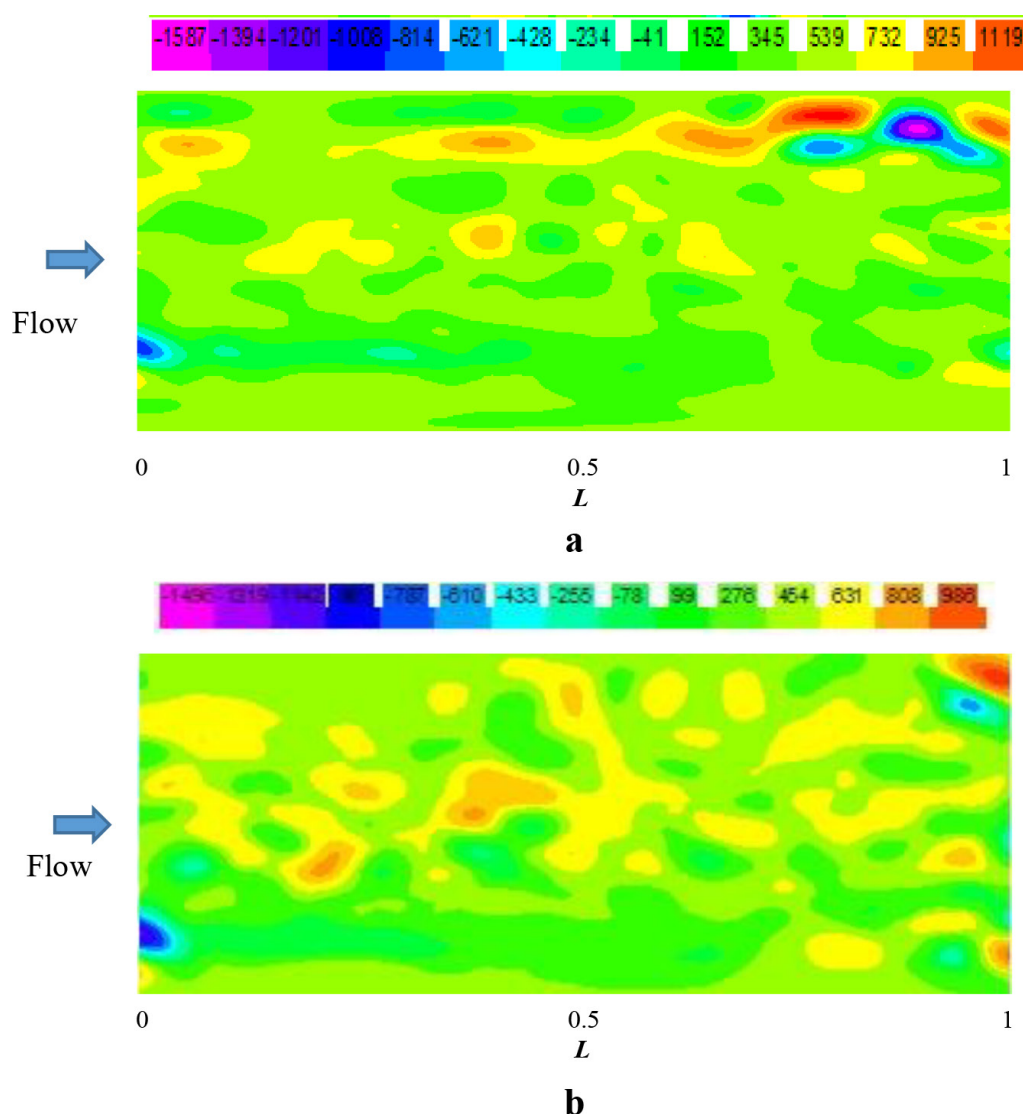


Fig. 6. Contours of vorticity from PIV results; a) For flow rate 0.033 kg s⁻¹; b) For flow rate 0.05 kg s⁻¹. Scale in s⁻¹.

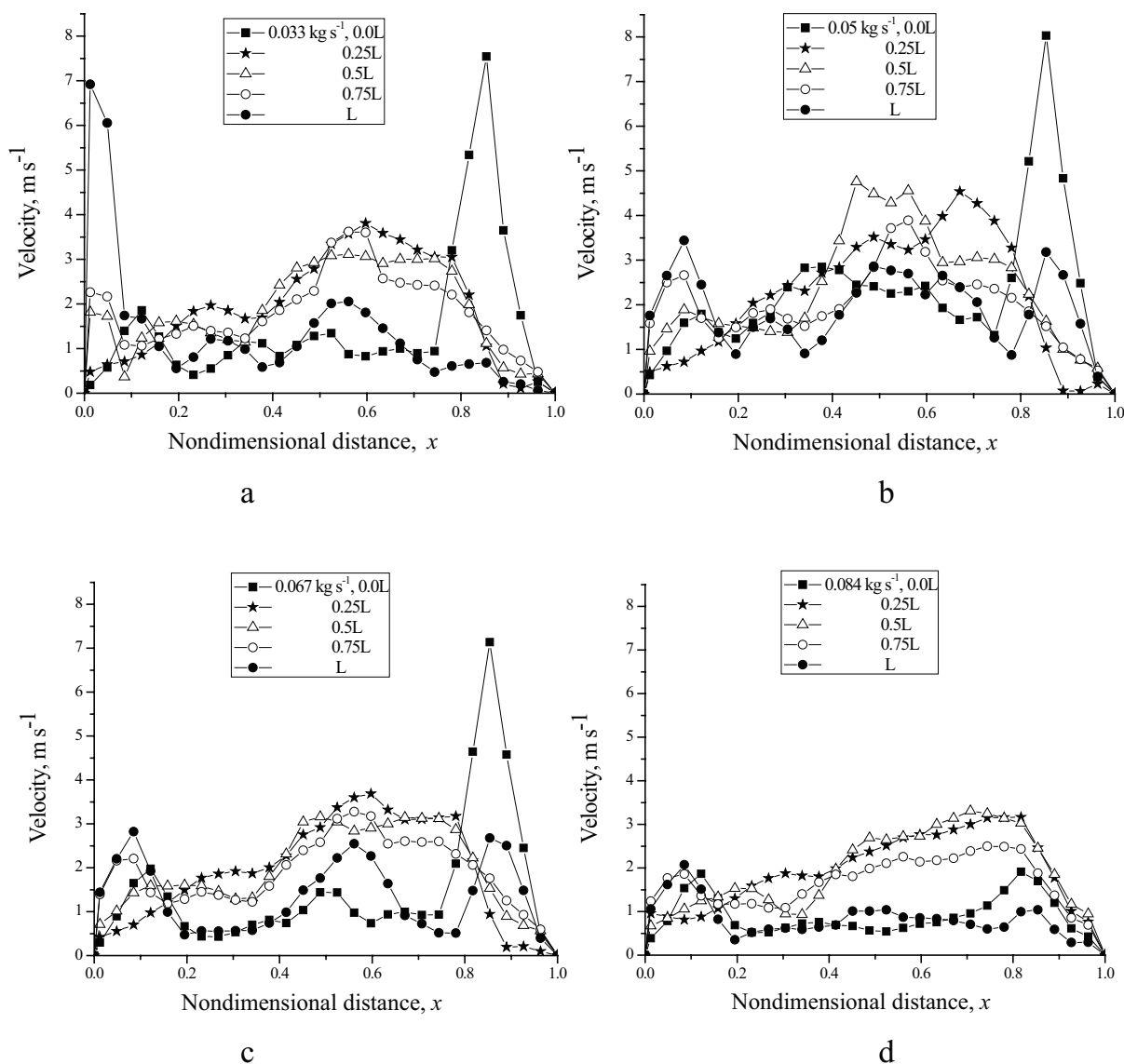


Fig. 7. Profiles of velocity from PIV for configuration 3, inlet pipe oriented perpendicular to reactor axis, for plane $y = 0.005$ m; a) For flow rate 0.033 kg s^{-1} ; b) For flow rate 0.05 kg s^{-1} ; c) For flow rate 0.067 kg s^{-1} ; d) For flow rate 0.084 kg s^{-1} .

original design. Therefore, a comparison of results from configurations 1 and 3 was analysed and the streamlines of both configurations is presented in Figs. 8a and b. The comparison extended to cover the design of the commercial reactor FM01-LC, which we see in Fig. 8c.

As observed, the change in configuration number 3 to produce a flow distribution with a small recirculating flow located after the discharge of the inflow. After this zone located in the beginning of the rectangular section L , the flow looks aligned better than obtained with the original configuration. Furthermore, this flow distribution is similar to the one obtained by the commercial electrochemical reactor FM01-LC, which has been simulated using the same program applied in the solution of configurations 1, 2 and 3. The effect of a manifold flow distributor confirms the popularity of this reactor.

3.4. Zone of electrochemical reaction

The numerical solution served to demonstrating that a simple geometry like configuration 3 can be a potential model of reactor compared against the FM01-LC reactor. To this end, flow distribution must warrant a reaction effectiveness. Therefore, in this section a comparison of reaction efficiency follows, emphasizing the magnitude of characteristic parameters that define the applicability of the present reactor.

Mass transport k_m in electrochemical reactors is a function of ionic interchange, which takes part in the Nernst layer. This region is of the same order of magnitude thickness as the boundary layer, near the cathode's surface [20]. An electrolyte with concentration $C_i = 10 \text{ mM CuSO}_4 \cdot 5\text{H}_2\text{O} + 100 \text{ mM H}_2\text{SO}_4$ useful in the process of electrodeposition was assumed as electroactive substance in contact with the cathode's surface. We present the results of total flux in the

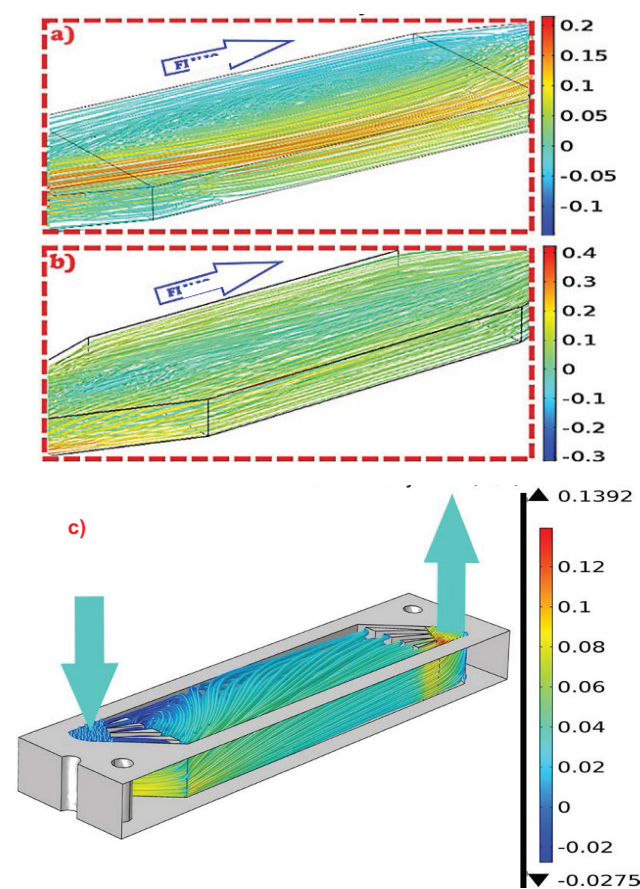


Fig. 8. Comparison of stream lines results from CFD; a) Configuration 1; b) Configuration 3; c) FM01-LC commercial reactor. Scale is in m s^{-1} .

cathode's surface in Fig. 9a–c. The results indicate that the recirculating flow affected the ionic flux in the configuration 1, which produces very low value, as observed in Fig. 9a. A region of very high activity located on $L = 0$ indicates high activity with the cathode's surface. Apart from this region, the ion interchange falls down. Compared against the FM01-LC reactor, which we observe in Fig. 9b, the effectivity of configuration 1 is very poor, because the FM01-LC presents a uniform ionic interchange as observed in almost all the cathode's surface.

This scenario is compared against the reactor of Configuration 3 proposed here, where this reactor looks like a normal reactor compared against the FM01-LC [21,22]. This is because the magnitude of total ion flux achieved by the reactor for configuration 3 is high and uniform, as seen in Fig. 8c.

3.5. Effect of inlet geometry on mass transport coefficient

4. Conclusions

A parallel plate electrochemical reactor was studied experimentally and numerically in order to demonstrate its reaction effectivity compared against a commercial

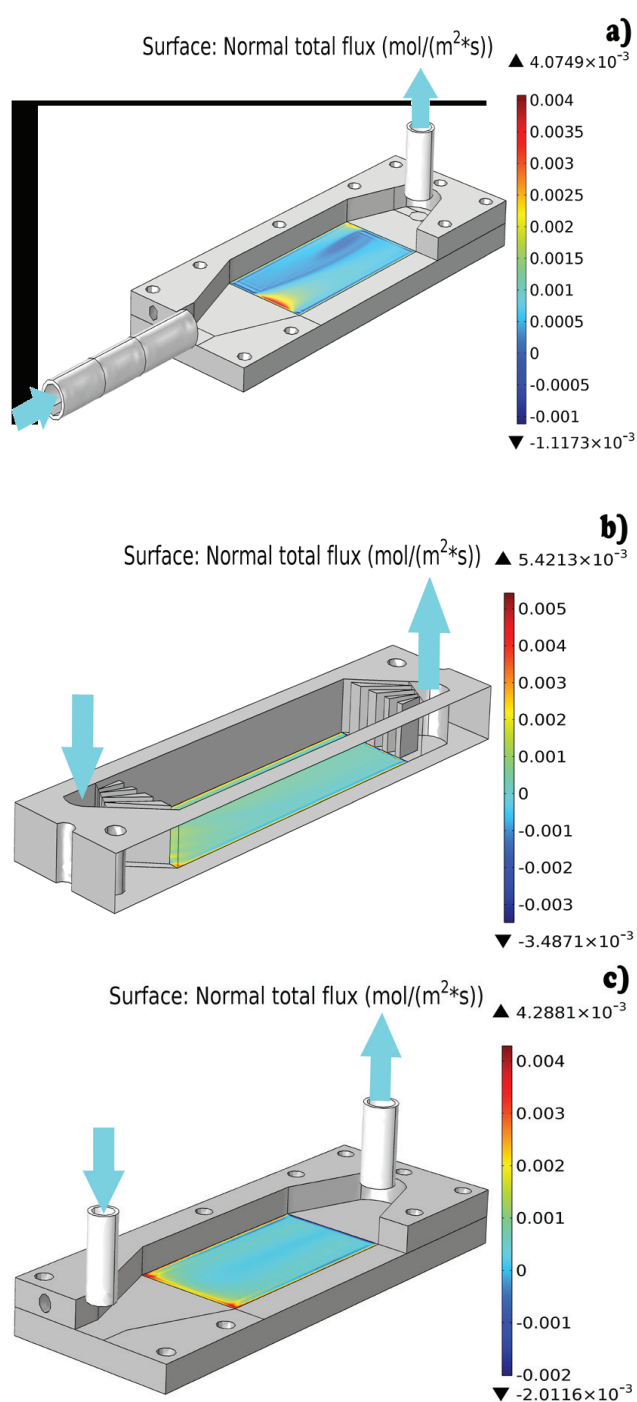
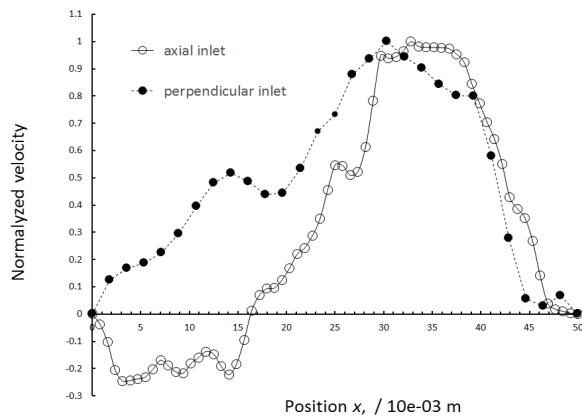
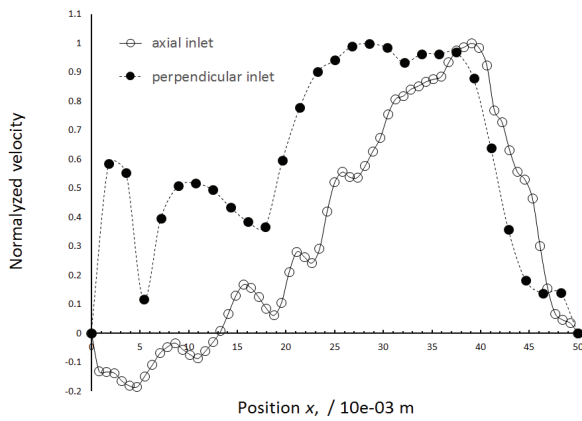


Fig. 9. Electrochemical reaction results from CFD; a) Configuration 1; b) Configuration 3; c) FM01-LC commercial reactor.

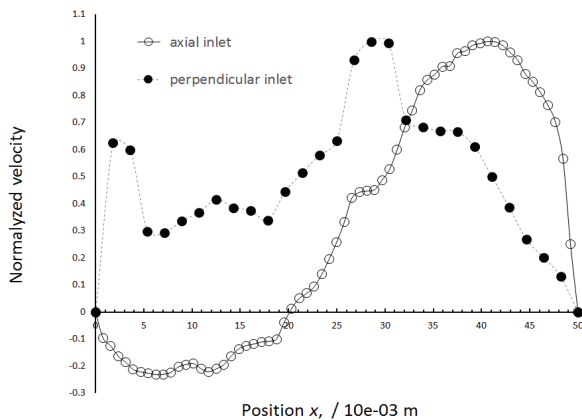
reactor. The modified reactor has an inlet pipe aligned in perpendicular direction to the reactor axis. An electrolyte with concentration $C_i = 10 \text{ mM CuSO}_4 \cdot 5\text{H}_2\text{O} + 100 \text{ mM H}_2\text{SO}_4$ with Reynolds number, $Re = 564$ to 1411 , based on the average velocity in the cross section area of the rectangular section of the reactor, and the separation distance between the parallel plates, was measured experimentally using PIV, and resolved numerically. The results showed



a



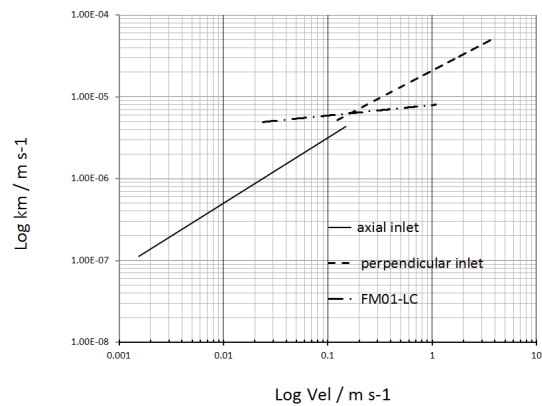
b



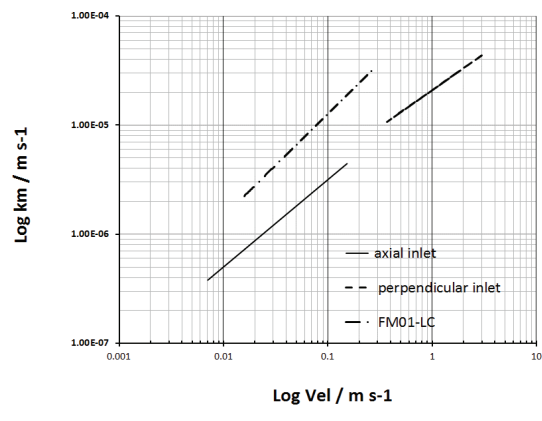
c

Fig. 10. Experimental results from PIV for original reactor design (axial inlet) compared against modified channel reactor (perpendicular inlet), for flow rate 2 kg s^{-1} and plane $y = 0.005 \text{ m}$; a) Position $L/4$; b) Position $L/2$; c) Position $3L/4$.

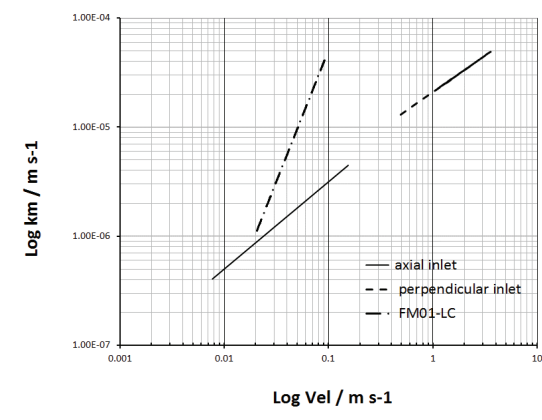
good agreement emphasizing the main characteristics of the flow distribution. With a full description of main flow several modifications to the inlet pipe configuration were studied varying the inlet diameter, the shape and the orientation of inlet pipe. The results showed that a nicely aligned



a



b



c

Fig. 11. Mass transport coefficient for original reactor design (axial inlet) compared against modified channel reactor (perpendicular inlet) and FM01-LC reactor, for flow rate 2 kg s^{-1} and plane $y = 0.005 \text{ m}$; a) Position $L/4$; b) Position $L/2$; c) Position $3L/4$.

flow like fully developed flow corresponding to configuration number 3 produce very good performance of electrochemical reactions. This reactor was compared against the FM01-LC electrolyser, which is provided with manifolds to stabilize the flow. The simplicity of the reactor's geometry

with inlet configuration perpendicular to the axial direction represents a competitive option for construction and costs, compared against the FM01-LC, given its high electrochemical reaction rate.

Acknowledgments

Authors thank the funds from the National Council for Science and Technology Conacyt, under grant number: CB2008-102167. G. Rodríguez thanks the financial support from postgraduate program-Conacyt during the PhD period.

References

- [1] F.C. Walsh, A first course in electrochemical engineering. The Electrochemical Consultancy, Romsey, UK, 1993.
- [2] C. Ponce de León, G.W. Reade, I. Whyte, S.E. Male, F.C. Walsh. Characterization of the reaction environment in a filterpress redox flow reactor. *Electrochim. Acta.*, 52 (2007) 5815–5823.
- [3] A. Frías-Ferrer, L. González-García, V. Saéz, C. Ponce de León, F.C. Walsh. The effects of manifold flow on mass transport in electrochemical filter-press reactors. *AIChE J.*, 54; 81 (2008) 1–823.
- [4] U.M. López-García, P.E. Hidalgo, J.C. Olvera, F. Castañeda, H. Ruíz, G. Orozco. The hydrodynamic behavior of a parallel plate electrochemical reactor, *Fuel*, 10 (2013) 162–170.
- [5] C. Ponce de León, D. Pletcher. Removal of formaldehyde from aqueous solutions via oxygen reduction using a reticulated vitreous carbon cathode cell. *J. Appl. Electrochem.*, 25 (1995) 307–314.
- [6] M.R.V. Lanza, R. Bertazzoli. Cyanide oxidation from wastewater in a flow electrochemical reactor, *Ind. Eng. Chem. Res.*, 41 (2002) 22–26.
- [7] A. Alvarez-Gallegos, D. Pletcher. The removal of low level organics via hydrogen peroxide formed in a reticulated vitreous carbon cathode cell, Part 1. The electrosynthesis of hydrogen peroxide in aqueous acidic solutions. *Electrochim. Acta*, 44 (1998) 853–861.
- [8] A.N. Colli, R. Toelzer, M.E.H. Bergmann, J.M. Bisang. Mass-transfer studies in an electrochemical reactor with a small interelectrode gap, *Electrochim. Acta*, 100 (2013) 78–84.
- [9] A.H. Herbst, P. Schlatter, D.S. Henningson, Simulations of turbulent flow in a plane asymmetric diffuser, *Flow Turbulence Combust.*, 79 (2007) 275–306.
- [10] G. Rodríguez Salazar, Methodology based on computational fluid dynamics for designing parallel plate electrochemical reactors. PhD Thesis, State Autonomous University of Morelos, Cuernavaca, July (2015).
- [11] G. Rodríguez, F.Z. Sierra-Espinosa, J. Teloxa, A. Álvarez, J.A. Hernández. Hydrodynamic design of electrochemical reactors based on computational fluid dynamics, *Desal. Water Treat.*, 57 (2016) 22968–22979.
- [12] G. Leticia Vázquez, A. Alvarez-Gallegos, F.Z. Sierra, C. Ponce de León, F.C. Walsh. CFD evaluation of internal manifold effects on mass transport distribution in a laboratory filter press flow cell, *J. Appl. Electrochem.*, 43 (2013) 453–465.
- [13] F.F. Rivera, C. Ponce de León, F.C. Walsh, J.L. Nava, The reaction environment in a filter-press laboratory reactor: the FM01-LC flow cell, *Electrochim. Acta.*, 161 (2015) 436–452.
- [14] R.D. Keane, R.J. Adrian. Theory of cross-correlation analysis of PIV Images, *J. Appl. Sci. Res.*, 49 (1992) 61–27.
- [15] B. Ganapathisubramani, E.K. Longmire, I. Marusic, S. Pophos. Dual-plane PIV technique to determine the complete velocity gradient in a turbulent boundary layer, *Exp. Fluids*, 39(2) (2005) 222–231.
- [16] J. Westerweel. On velocity gradients in PIV interrogation, *Exp. Fluids*, 44(5) (2008) 831–842.
- [17] Dantec Dynamics, Flow Manager User's guide, 2009.
- [18] J. Ferziger, M. Peric. Computational methods for fluid dynamics, Springer, Germany, 1996.
- [19] B.E. Launder, D.B. Spalding, The numerical computation of turbulent flows, *Comp. Methods Appl. Mech. Eng.*, 3 (1974) 269–289.
- [20] H. Schlichting, K. Gersten. Boundary layer theory, 8th ed. Springer-Verlag, Berlin-Heidelberg, 2000.
- [21] G. Nelissen, van den B. Bossche, J. Deconink, A. van Theemsche, C.D. Adrian, Laminar and turbulent mass transfer simulations in parallel plate reactor, *J. App. Electrochem.*, 33 (2003) 863–873.
- [22] E.P. Rivero, F.F. Rivera, M.R. Cruz-Díaz, E. Mayen, I. González. Numerical simulation of mass transport in a filter press type electrochemical reactor FM01-LC: Comparison of predicted and experimental mass transfer coefficient. *Chem. Eng. Res. Des.*, 90 (2012) 1969–1978.
- [23] F. Goodridge, K. Scott, *Electrochemical process engineering: A guide to the design of electrolytic plant.* Plenum Pres, New York, 1995.